IEEE Access
Multidisciplinary | Rapid Review | Open Access Journal

Received February 12, 2019, accepted March 8, 2019, date of publication March 12, 2019, date of current version April 1, 2019.

Digital Object Identifier 10.1109/ACCESS.2019.2904612

Resource Allocation for Symbiotic Radio System With Fading Channels

HUAYAN GUO[1,2], (Member, IEEE), YING-CHANG LIANG[2], (Fellow, IEEE), RUIZHE LONG[1,2], (Student Member, IEEE), SA XIAO[1,2], (Member, IEEE), AND QIANQIAN ZHANG[1,2], (Student Member, IEEE)

[1]National Key Laboratory of Science and Technology on Communications, University of Electronic Science and Technology of China, Chengdu 611731, China
[2]Center for Intelligent Networking and Communications (CINC), University of Electronic Science and Technology of China, Chengdu 611731, China

Corresponding author: Ying-Chang Liang (liangyc@ieee.org)

This work was supported by the National Natural Science Foundation of China under Grant U1801261, Grant 61631005, and Grant 61571100.

ABSTRACT In this paper, we investigate the resource allocation problem for the symbiotic radio system, in which the passive backscatter transmission is parasitic in the primary transmission, and the cooperative receiver simultaneously detects the signals transmitted from the active primary transmitter (PT) and the backscatter device (BD). In particular, channel fading is considered, and the ergodic weighted sum rate of the primary and backscatter transmissions is maximized by jointly optimizing the transmit power at the PT and the reflection coefficient at the BD under either long-term or short-term transmit-power constraint over the fading states. Two practical transmission setups are considered, where the relationship between the primary and backscatter transmissions is either commensal or parasitic. For the commensal setup, we fix the reflection coefficient as the maximum value and derive the optimal power allocation scheme based on the standard convex optimization procedure. For the parasitic setup, the weighted sum-rate maximization problem is non-convex, and we resort to the concave–convex procedure to derive a suboptimal solution. Simulation results demonstrate that in the commensal setup, the BD may realize transmission while causing no harmful interference to the primary system; in the parasitic setup, a higher backscatter data rate can be achieved through slightly sacrificing the primary transmission rate.

INDEX TERMS Internet of Things, ambient backscatter communications, symbiotic radio, ergodic rate, spectrum sharing, fading channel.

I. INTRODUCTION

A. BACKGROUNDS

Symbiotic radio has emerged as a promising technology for next-generation *Internet of Things* (IoT), in which passive IoT transmissions are parasitic in primary communication systems (e.g., cellular, TV, or WiFi systems) [1]–[3]. In particular, the IoT device in symbiotic radio system, also referred to as the *backscatter device* (BD), transmits information over the incident primary signal via backscatter modulation without requiring active *radio-frequency* (RF) components [4]–[7]. In contrast to the traditional backscatter communication system, such as *radio-frequency-identification* (RFID) system, which relies on dedicated radio spectrum resources and RF sinusoidal carriers, the BD in symbiotic radio system shares the same radio spectrum and the same RF source with the primary system, resulting in higher spectrum efficiency and more flexible network deployment [8]–[11].

The most famous paradigm for the symbiotic radio is the *ambient backscatter communication* (AmBC) system [12]–[14]. Fig. 1(a) illustrates the conventional AmBC system, in which the IoT receiver receives signal from both the *primary transmitter* (PT) and the BD. Due to the lack of coordination, the IoT receiver treats the direct-link signal (i.e., signal transmitted directly from the PT) as interference, and energy detector is commonly adopted to extract BD's messages [14]–[16]. However, the signal backscattered from BD, also referred to as the backscatter signal, is much weaker than the direct-link interference [6]. As a result, the energy detector suffers from severe error floor problem, and the

The associate editor coordinating the review of this manuscript and approving it for publication was Bora Onat.

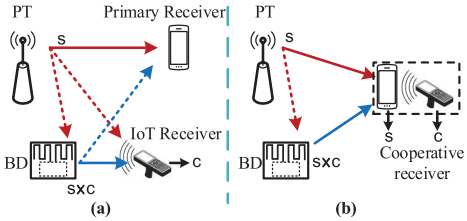

Fig. 1. Two types of symbiotic radio systems: (a) Conventional AmBC system; (b) AmBC system with cooperative receiver.

transmission rate and coverage for conventional AmBC are quite limited [16], [17]. Due to that, the conventional AmBC is mainly considered as a backup communication technique for the batteryless IoT devices which is applied when the harvested power cannot support the high-speed active transmission [18]–[22].

There are several techniques proposed in the literature to suppress the direct-link interference using, e.g., receive beamforming with multiple antennas [17], or special BD waveform design [23]. Another interesting approach is the cooperative receiver, as shown in Fig. 1(b), which integrates the IoT receiver with the primary receiver. Then, both the primary signal and BD's signal are jointly decoded by the cooperative receiver, and the direct-link interference problem is overcome by the joint decoding algorithm [24]. The cooperative receiver technique enables the existing network infrastructure to support the passive IoT communications via software upgrade. One application scenario is the wearable communication, in which the wearable devices, e.g., the medical sensors and the fitness trackers, send messages to the smart phone via backscattering the primary signal transmitted from the cellular base-station or WiFi access point to the smart phone [25]. In this case, the smart phone needs to decode the messages from both the primary transmitter and the backscatter device, i.e., the primary receiver and secondary receiver combined. Another application is smart home, in which the home sensors send messages to the WiFi access point via backscattering the WiFi signal transmitted from smart devices to the WiFi access point. In this case, the WiFi access points recovers messages from the smart devices as well as the home sensors.

B. RELATED WORKS, MOTIVATIONS, AND CONTRIBUTIONS

The idea of the cooperative receiver was first presented in [24], in which the bit error rates for both primary and backscatter transmissions were derived. In [26], a constellation learning based detector was designed which jointly realized semi-blind channel estimation and symbol detection without requiring pilots from PT. The achievable rates of the primary and backscatter transmissions were analyzed in [7], in which BD was assumed to employ the Gaussian codebook, and the PT was assumed to employ the Wyner polyphase coding or the Gaussian codebook. Liu *et al.* [27] derived the achievable rates when BD employed binary modulation. The term of the ''symbiotic radio'' was firstly presented in [1], in which a backscatter transmission is parasitic with a primary transmission, and the achievable rate tradeoff between the primary and backscatter transmissions was realized by transmit beamforming. Then, in [2] and [3], the concept of the symbiotic radio is introduced to the full-duplex communication system and the non-orthogonal multiple access system, respectively. However, all these works mainly focus on the *additive white Gaussian noise* (AWGN) channel or a fixed fading state of the fading channels, while the impact of channel fading has not been addressed before.

In this paper, we investigate the resource allocation problem for the symbiotic radio system which employs the cooperative receiver. Note that, we only focus on the wireless communication problem, and the BD does not harvest power from the PT. The ergodic weighted sum rate of the primary and backscatter transmissions is maximized over the channel fading states. We point out the spectrum growth phenomenon for the backscatter transmission of symbiotic radio system: the bandwidth of the backscatter signal is generally larger than the receive filter bandwidth of the cooperative receiver, and distortion may happen when the backscatter signal goes through the receive filter of the cooperative receiver. Then, two practical transmission setups are proposed to alleviate this problem:

- The first one is the commensal setup, in which the symbol period for BD transmission is much longer than that of the primary transmission, so that the growth spectrum is negligible, and then the primary signal and BD's signal are jointly decoded at the cooperative receiver.
- The second one is the parasitic setup, in which the BD transmission is perfectly synchronized with the primary transmission, so that there is no spectrum growth even though the BD transmission and primary transmission have the same symbol period. In this setup, *successive interference cancellation* (SIC) is employed. The primary signal is decoded first while the backscatter signal is treated as interference, and then the BD's signal is decoded after removing the primary signal.

For each transmission setup, the closed-form expressions of the instantaneous achievable rates are derived while both the PT and the BD are assumed to employ the Gaussian codebook. Based on that, we formulate the joint transmit power allocation and reflection coefficient adjustment problem. Two types of transmit-power constraint are considered. One is the *long-term* (LT) transmit-power constraint that regulates the average transmit power across all the fading states at the PT. The other is the *short-term* (ST) transmit-power constraint that limits the instantaneous transmit power at each fading state to be below a certain threshold. For the commensal setup, we first derive the optimal reflection coefficient, and then the transmit power is optimized. For the parasitic setup, the joint power allocation and reflection coefficient adjustment problem is non-convex, and we resort to the concave-convex procedure to transform it into a sequence of convex optimization problems, and then adopt Lagrange dual decomposition to tackle them.

The main contributions of this work are summarized as follows:

- Firstly, this paper is one of the early attempts to study resource allocation problems for symbiotic radio system considering the impact of channel fading. Two practical transmission setups are investigated, both of which can overcome the spectrum growth phenomenon.
- Secondly, for the commensal setup, the instantaneous achievable rates of the primary and backscatter transmissions are tightly approximated by closed-form expressions. Based on that, the optimal resource allocation solutions for the ergodic weighted-sum-rate maximization problem are derived. It is further shown that, the backscatter signal in this setup provides an additional beneficial signal path for the primary transmission instead of harmful interference.
- Thirdly, for the parasitic setup, the achievable rates given certain channel fading states are derived based on SIC technique. The resource allocation problem is non-convex, and we propose an iterative method to solve it sub-optimally by applying the concave-convex procedure. Simulation results have verified the effectiveness of the proposed method.

The rest of the paper is organized as follows. Section II establishes the system model. In Section III, the commensal setup is investigated, and the optimal transmit power and reflection coefficient for each fading state are derived. Then in Section IV, the parasitic setup is investigated, and the non-convex optimization problem is solved by applying the concave-convex procedure. Simulation results are provided in Section V and conclusions are drawn in Section VI.

The main notations in this paper are listed as follows: The lowercase, boldface lowercase, and boldface uppercase letters such as t, $\mathbf{t}$, and $\mathbf{T}$ denote the scalar, vector, and matrix, respectively. $|t|$ denotes the absolute value of t. $\|\mathbf{t}\|$ denotes the norm of vector $\mathbf{t}$. $\mathcal{CN}(\mu, \sigma^2)$ denotes the *circularly symmetric complex Gaussian* (CSCG) distribution with mean μ and variance σ^2. $\mathbb{E}[\cdot]$ denotes the statistical expectation. t^* denotes the conjugate of t. $\mathbf{T}^{\mathrm{T}}$ and $\mathbf{T}^{\mathrm{H}}$ denotes the transpose and conjugate transpose of matrix $\mathbf{T}$, respectively. Finally, the list of abbreviations commonly appeared in this paper is given in Table 1.

TABLE 1. List of abbreviations.

Abbreviation	Description
IoT	Internet of Things
AmBC	Ambient Backscatter Communication
BD	Backscatter Device
PT	Primary Transmitter
CRx	Cooperative Receiver
AWGN	Additive White Gaussian Noise
CSCG	Circularly Symmetric Complex Gaussian
SIC	Successive Interference Cancellation
LT	Long-Term
ST	Short-Term
SNR	Signal-to-Noise Ratio
SINR	Signal-to-Interference-plus-Noise Ratio
PDF	Probability Density Function

II. SYSTEM MODEL

A. CHANNEL ASSUMPTIONS

A basic symbiotic radio system with cooperative receiver is depicted in Fig. 2, which consists of an active PT, a semi-passive BD, and a *cooperative receiver* (CRx). The CRx receives and decodes both the PT's signal and the BD's signal. A block-fading channel model is assumed for all the channels involved. During each transmission block, the instantaneous channel coefficients of the direct channel (i.e., the PT-CRx channel) and the backscatter channel (i.e., the PT-BD-CRx channel) are denoted by h_1 and h_2, respectively. In addition,

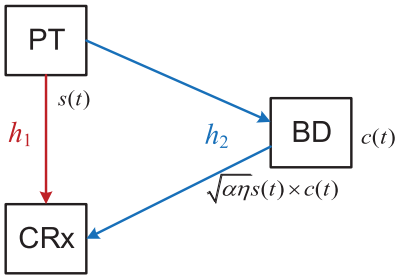

Fig. 2. The symbiotic radio system with a cooperative receiver.

h_1 and h_2, are assumed to be ergodic and stationary, and perfect channel state information on h_1 and h_2 is assumed to be available to all the three nodes in the symbiotic radio system [7], [24], [27].[1] For simplicity, h_1 and h_2 are normalized in this paper, i.e., $\mathbb{E}[|h_1|] = \mathbb{E}[|h_2|] = 1$.

B. RECEIVED SIGNALS FOR TWO TRANSMISSION SETUPS

Since we are interested in the information-theoretic limits of symbiotic radio system, we assume that the Gaussian codebook is used by the PT and the BD.

The primary signal is expressed as:

$$s(t) = \sum_n s_n g_s(t - nT_s), \tag{1}$$

where $s_n \sim \mathcal{CN}(0, 1)$ denotes the n-th symbol to be transmitted, T_s is the symbol duration, and $g_s(t)$ is the pulse-shaping filter (e.g., the square-root raised-cosine filter). Similarly, the BD's signal can be expressed as

$$c(t) = \sum_n c_n g_c[t - (n + \tau)T_c], \tag{2}$$

where $c_n \sim \mathcal{CN}(0, 1)$ is the n-th symbol, T_c is the symbol duration, $g_c(t)$ is the rectangular pulse-shaping filter, and τ is the symbol delay between s_n and c_n.

[1]The channel state information can be obtained by the classic channel training, estimation, and feedback mechanisms. The impact of channel estimation imperfection is beyond the scope of this paper.

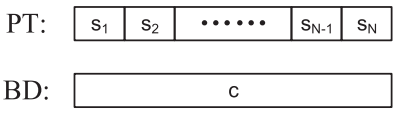

Fig. 3. Illustration of s and c in the commensal setup.

The signal transmitted from BD to CRx is equivalent to multiplying $c(t)$ by $s(t)$ [6]. The received signal at CRx is the summation of the signal from PT and the signal from BD:

$$r(t) = \sqrt{P}h_1 s(t) + \sqrt{P\alpha\eta}h_2 c(t)s(t) + u(t), \tag{3}$$

where P is the transmit power of PT, $0 \leq \alpha \leq 1$ is the reflection coefficient of BD, η denotes the double-fading channel loss due to backscattering [6], and $u(t)$ is the additive noise. Typically, η is a small number, and so the backscatter link is much weaker than the direct link [17].

The match filter at CRx is designed for the primary system. The summation signal $r(t)$ in (3) goes through the match filter $g_s(t)$, yielding

$$y(t) = \int_{-\infty}^{\infty} g_s(t-\varsigma)r(\varsigma)d\varsigma. \tag{4}$$

The received digital-domain signal y_n can be obtained by sampling $y(t)$ at interval nT_s.

In general, the bandwidth of the backscatter signal $c(t)s(t)$ in (3) is the summation of the bandwidth of $c(t)$ and the bandwidth of $s(t)$. As a result, when $c(t)s(t)$ goes through the match filter, the BD's signal cannot be decoded due to the signal distortion, which is the co-called spectrum growth phenomenon. In practice, there are two methods to alleviate this problem, resulting in two transmission setups.

1) COMMENSAL SETUP

In this setup, c_n has a much longer symbol duration than s_n. We assume that $T_c = NT$, where N is referred to as the spreading factor. Then, when N is very large, the bandwidth of c_n is negligible.

During one BD symbol, the transmission signal of the primary system is a vector, $\mathbf{s} = [s_1, \cdots, s_N]$, as illustrated in Fig. 3. The received signal of the CRx during one symbol duration of the BD can be written as

$$\mathbf{y} = \sqrt{P}h_1\mathbf{s} + \sqrt{P\alpha\eta}h_2 c\mathbf{s} + \mathbf{u}, \tag{5}$$

where $\mathbf{y} = [y_1, \cdots, y_N]$ and $\mathbf{u} \sim \mathcal{CN}(0, \mathbf{I}_N)$. Also note that, in this setup, as N goes large, the detection performance degrades negligibly for the imperfect synchronization with $|\tau| < 1$ [27]. Thus the synchronization requirement is not rigid for this setup.

2) PARASITIC SETUP

In fact, if we have $\tau = 0$, which means perfect synchronization between the primary transmission and BD transmission, the spectrum growth phenomenon also disappears. In this case, c_n may have the same data rate as s_n, i.e., $N = 1$. The received signal of the CRx is written as

$$y_n = \sqrt{P}h_1 s_n + \sqrt{P\alpha\eta}h_2 s_n c_n + u_n, \tag{6}$$

where $u_n \sim \mathcal{CN}(0, 1)$ is the additive noise.

It is worth noting that, for the parasitic setup, the decoding *signal-to-noise ratio* (SNR) for c_n is very low, and thus in this case, although the BD adopts simple binary modulation as investigated in [27], the achievable rate can be very close to that obtained by Gaussian codebook.[2] However, for the commensal setup, the decoding SNR increases owing to the large spreading factor N, and high-order backscatter modulations are required to achieve the Gaussian-codebook data rate. The high-order backscatter modulations have been investigated recently in many studies, such as the 4-PAM in [28], MPSK in [29], and 16-QAM in [30].

C. TRANSMIT POWER CONSTRAINTS

Denote $\mathbf{v} = [h_1, h_2]$. Our objective is to design the resource allocation policy on the transmit power $P(\mathbf{v})$ and the reflection coefficient $\alpha(\mathbf{v})$ to maximize the ergodic weighted sum rate of the symbiotic radio system.

In this paper, we assume that the reflection coefficient of BD can be adjusted in every transmission block, which satisfies

$$0 \leq \alpha(\mathbf{v}) \leq 1, \quad \forall \mathbf{v}. \tag{7}$$

The transmit power should satisfy

$$P(\mathbf{v}) \geq 0, \quad \forall \mathbf{v}. \tag{8}$$

Besides that, we further consider two types of power constraints at the PT. The first is the ST power constraint (also known as peak transmit power constraint), which is represented by

$$P(\mathbf{v}) \leq P_{\mathrm{ST}}, \quad \forall \mathbf{v}. \tag{9}$$

The second is the LT power constraint (also known as average transmit power constraint), which is represented by

$$\mathbb{E}[P(\mathbf{v})] \leq P_{\mathrm{LT}}. \tag{10}$$

III. COMMENSAL SETUP

In this section, we investigate the ergodic weighted-sum-rate maximization problem for the commensal setup. We first analyze the instantaneous achievable rate given channel coefficients h_1 and h_2, the transmit power P and the reflection coefficient α. Then, the resource allocation policy is investigated for the ST/LT power constraint.

[2]We will introduce a SNR-loss factor to indicate the SNR gap to the information theoretical channel capacity due to the use of practical coding and modulation when we derive the achievable rates.

A. INSTANTANEOUS ACHIEVABLE RATE ANALYSIS

In the commensal setup, N is a large number. Based on [13] and [27], the CRx may jointly decode $\mathbf{s}$ and c via a common decoder, and the maximum achievable rates of $\mathbf{s}$ and c are represented as follows

$$R_{\mathrm{s}} = I(\mathbf{s}; \mathbf{y}|c), \tag{11}$$

$$R_{\mathrm{c}} = I(c; \mathbf{y}|\mathbf{s}). \tag{12}$$

When decoding $\mathbf{s}$ for given c, the received signal can be represented as

$$\mathbf{y} = \sqrt{P}\left(h_1 + \sqrt{\alpha\eta}h_2 c\right)\mathbf{s} + \mathbf{u}. \tag{13}$$

The instantaneous SNR of decoding $\mathbf{s}$ for given c is

$$\gamma_{\mathbf{s}|c} = P\left|h_1 + \sqrt{\alpha\eta}h_2 c\right|^2. \tag{14}$$

Let $\kappa_1 = \left|h_1 + \sqrt{\alpha\eta}h_2 c\right|^2$. Since BD adopts Gaussian codebook, κ_1 follows the non-central chi-square distribution with *probability density function* (PDF):

$$f_{\kappa_1}(x) = \frac{1}{\alpha\eta|h_2|^2} e^{-\frac{|h_1|^2+x}{\alpha\eta|h_2|^2}} I_0\left(\frac{2|h_1|}{\alpha\eta|h_2|^2}\sqrt{x}\right), \tag{15}$$

where $I_0(\cdot)$ is the modified Bessel function of the first kind with order zero. Then the achievable rate of the primary system is

$$\begin{aligned} R_{\mathrm{s}} &= \mathbb{E}_c\left[\log_2(1+\gamma_{\mathbf{s}|c}\Gamma_{\mathrm{s}})\right] \\ &= \mathbb{E}_{\kappa_1}\left[\log_2(1+\Gamma_{\mathrm{s}}P\kappa_1)\right] \\ &= \int_0^\infty \log_2(1+\Gamma_{\mathrm{s}}Px) f_{\kappa_1}(x)\,\mathrm{d}x, \end{aligned} \tag{16}$$

where $0 \le \Gamma_{\mathrm{s}} \le 1$ is the SNR-loss factor which indicates the SNR gap to the information theoretical channel capacity, due to the use of practical coding and modulation for the linear Gaussian channel [31]. As the PT employs Gaussian codebook, we have $\Gamma_{\mathrm{s}} = 1$, and thus we omit it for simplicity in the rest of this paper.

From (5), when decoding c for given $\mathbf{s}$, the known additive term $\sqrt{P}h_1\mathbf{s}$ can be removed firstly, and then the received signal becomes

$$\mathbf{y} = \sqrt{P\alpha\eta}h_2 c\mathbf{s} + \mathbf{u}. \tag{17}$$

Then we perform maximal ratio combining using $\mathbf{s}$. The instantaneous SNR of decoding c for given $\mathbf{s}$ is

$$\gamma_{c|\mathbf{s}} = P\alpha\eta|h_2|^2\|\mathbf{s}\|^2. \tag{18}$$

Let $\kappa_2 = \frac{1}{N}\|\mathbf{s}\|^2$. κ_2 follows a central chi-square distribution with $2N$ degrees of freedom, whose PDF is

$$f_{\kappa_2}(x) = \frac{N^N}{\Gamma(N)} x^{N-1} e^{-Nx}, \tag{19}$$

where $\Gamma(N) \triangleq (N-1)!$ is the gamma function. Then the achievable rate of BD transmission is

$$\begin{aligned} R_{\mathrm{c}} &= \mathbb{E}_{\mathbf{s}}\left[\frac{1}{N}\log_2(1+\gamma_{c|\mathbf{s}}\Gamma_{\mathrm{c}})\right] \\ &= \mathbb{E}_{\kappa_2}\left[\frac{1}{N}\log_2(1+\Gamma_{\mathrm{c}}NP\alpha\eta|h_2|^2\kappa_2)\right] \\ &= \int_0^\infty \frac{1}{N}\log_2(1+\Gamma_{\mathrm{c}}NP\alpha\eta|h_2|^2 x) f_{\kappa_2}(x)\,\mathrm{d}x, \end{aligned} \tag{20}$$

where $0 \le \Gamma_{\mathrm{c}} \le 1$ is the SNR gap to the information theoretical channel capacity for BD transmission. When BD employs Gaussian codebook, we have $\Gamma_{\mathrm{c}} = 1$ and thus it can also be omitted.[3]

However, both R_{s} in (16) and R_{c} in (20) are intractable due to the complicated integral expressions. Fortunately, R_{s} and R_{c} can be well approximated by simple expressions based on the fact that both N and P are relatively large in typical application scenarios.

In the commensal setup, N is generally a large number. It is known that, the mean of κ_2 is equal to 1, and the variance of κ_2 becomes negligible as N approaches to infinity. Thus we have $R_{\mathrm{c}} \approx R_{\mathrm{c}}^{\circ}$ where:

$$\begin{aligned} R_{\mathrm{c}}^{\circ} &= \frac{1}{N}\log_2(1+NP\alpha\eta|h_2|^2\mathbb{E}[\kappa_2]) \\ &= \frac{1}{N}\log_2(1+NP\alpha\eta|h_2|^2). \end{aligned} \tag{21}$$

In addition, P is usually high in the typical application scenarios of the symbiotic radio system. Then we have the following proposition.

Proposition 1: When P approaches to infinity, R_s in (16) *can be approximated with a closed-form expression as follows:*

$$R_s^{\circ} = \log_2(1+P|h_1|^2) - Ei\left(-\frac{|h_1|^2}{\alpha\eta|h_2|^2}\right)\log_2 e, \tag{22}$$

where $Ei(x) \triangleq -\int_{-x}^{\infty}\frac{1}{a}e^{-a}da$ is the exponential integral.

Proof: See Appendix A. ∎

We verify the approximation accuracy of R_{c}° and R_{s}° in Fig. 4(a) and Fig. 4(b), respectively, in which h_1 and h_2 are Rayleigh fading channels and $\eta = -20$ dB. From Fig. 4(a), R_{c}° can well approximate R_{c} when N is larger than 20. From Fig. 4(b), R_{s}° shows high approximation precision when P is larger than 0 dB. Therefore, for ease of analysis, we use the approximated expressions in (21) and (22) to replace the complicated expressions in (20) and (16) for R_{c} and R_{s}, respectively.

Theorem 1: The optimal reflection coefficient for the commensal setup is $\alpha = 1$, and then R_s and R_c become functions of P:

$$R_s = \log_2(1+P|h_1|^2) - Ei\left(-\frac{|h_1|^2}{\eta|h_2|^2}\right)\log_2 e, \tag{23}$$

$$R_c = \frac{1}{N}\log_2(1+NP\eta|h_2|^2). \tag{24}$$

Proof: From (21) and (22), both R_{c} and R_{s} are monotonic increasing function of α. Thus the theorem is proved. ∎

[3]Noted that, the values of Γ_{s} and Γ_{c} will not affect the structure of the optimization problems formulated and the solutions obtained in this paper. Actually, Γ_{s} and Γ_{c} can be combined into the channel gains of the direct link and the backscatter link, respectively, practical coding and modulation cases.

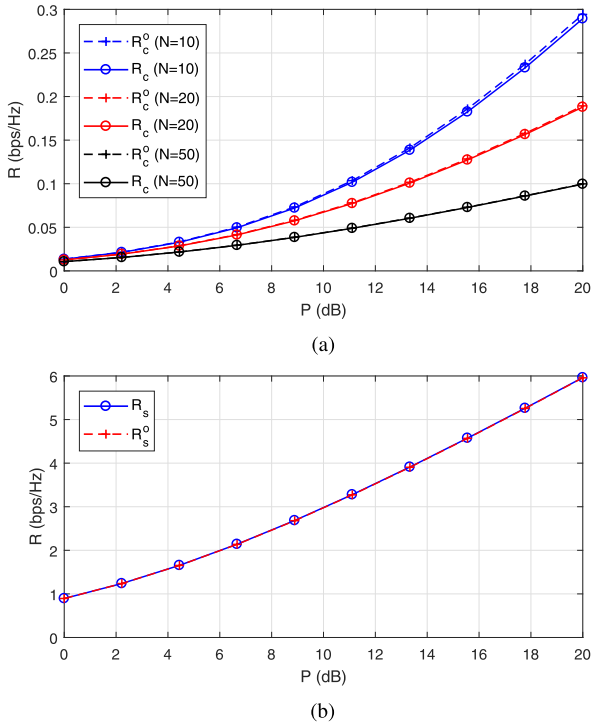

Fig. 4. Checking the approximation accuracy of R_c° and R_s° when h_1 and h_2 are Rayleigh fading channels and $\eta = -20$ dB. (a) Comparison of R_c and R_c° for different N. (b) Comparison of R_s and R_s° for different P.

Remark: The first term in (23), i.e., $\log_2(1+P|h_1|^2)$, is the data rate achieved by the primary system when BD is absent. Meanwhile, the second term $-\text{Ei}\left(-\frac{|h_1|^2}{\eta|h_2|^2}\right)\log_2 e$ is always larger than zero. Therefore, the primary transmission will not be interfered by the BD transmission. In addition, the signal backscatter from the BD even provides an additional beneficial signal path which can slightly enhance the primary transmission. That is the reason why this setup is referred to as ''commensal''.

B. ERGODIC WEIGHTED SUM RATE MAXIMIZATION

The remaining task is to design the optimal power allocation policy $P(\mathbf{v})$. From Section II-C, we have two power constraint sets:

$$\mathcal{F}_1 \triangleq \{P(\mathbf{v}):\ (8),\ (9)\}, \tag{25}$$
$$\mathcal{F}_2 \triangleq \{P(\mathbf{v}):\ (8),\ (10)\}. \tag{26}$$

The maximum ergodic weighted sum rate can be obtained by solving the following optimization problem:

$$\max_{P(\mathbf{v})\in\mathcal{F}} \ \mathbb{E}[(1-w)R_s + wR_c], \tag{27}$$

where $0 \le w \le 1$ is the weighting factor, $\mathcal{F} \in \{\mathcal{F}_1, \mathcal{F}_2\}$ is the constraint set, and the expectation is taken over v.

1) ST POWER CONSTRAINT

In this case, $\mathcal{F}$ in (27) becomes $\mathcal{F}_1$. From (23) and (24), both R_s and R_c are increasing functions of P. Therefore, the weighted sum rate is maximized by transmitting at the maximum instantaneous power:

$$P(\mathbf{v}) = P_{\text{ST}}. \tag{28}$$

2) LT POWER CONSTRAINT

In this case, $\mathcal{F}$ in (27) becomes $\mathcal{F}_2$. The optimization problem is expressed as follows:

$$\text{(P0)} \ \max_{P(\mathbf{v})} \ \mathbb{E}[(1-w)R_s + wR_c]$$
$$\text{s.t. } P(\mathbf{v}) \ge 0, \quad \forall \mathbf{v}$$
$$\mathbb{E}[P(\mathbf{v})] \le P_{\text{LT}}.$$

From (23) and (24), both R_s and R_c are the concave functions of P. Therefore, the weighted-sum-rate maximization problem is convex. The partial Lagrangian of (P0) is expressed as

$$\mathcal{L}\big(P(\mathbf{v}),\lambda\big) = \mathbb{E}[(1-w)R_s + wR_c] - \lambda\big(\mathbb{E}_{\mathbf{v}}[P(\mathbf{v})] - P_{\text{LT}}\big), \tag{29}$$

where $\lambda \ge 0$ is the dual variable associated with the constraint $\mathbb{E}[P(\mathbf{v})] \le P_{\text{LT}}$. The Lagrangian dual function is given by

$$\mathcal{G}(\lambda) = \max_{p(\mathbf{v})\ge 0} \mathcal{L}\big(P(\mathbf{v}),\lambda\big). \tag{30}$$

The dual problem is accordingly defined as

$$\min_{\lambda\ge 0} \ \mathcal{G}(\lambda). \tag{31}$$

It can be verified that, the Slater's condition [32] is satisfied and thus the duality gap is indeed zero. Therefore, solving the above dual problem is equivalent to solving the original problem (P0).

Theorem 2: The optimal P given λ and $\mathbf{v}$ is

$$P^*(\lambda,\mathbf{v}) = \left(\frac{\sqrt{b_2}-b_1}{2N\eta|h_1h_2|^2}\right)^+, \tag{32}$$

where $b_1 = |h_1|^2 + N\eta|h_2|^2 - \frac{(1-w+wN)\eta|h_1\ h_2|^2}{\lambda}\log_2 e$ *and* $b_2 = b_1^2 - 4\,N\eta|h_1\ h_2|^2(1 - \frac{w|h_1|^2+(1-w)\eta|h_2|^2}{\lambda}\log_2 e)$.

Proof: For a fixed λ, the dual function in (30) can be decomposed into a series of sub-dual-functions each for one fading state. For a particular fading state, the problem is shown as follows:

$$\text{(P0a)} \ \max_{P\ge 0} \ (1-w)R_s + wR_c - \lambda P. \tag{33}$$

After solving (P0a) for all the fading states, λ can be determined by solving $\mathbb{E}[P(\mathbf{v})] = P_{\text{LT}}$.

Let the first-order derivative of the objective function of (P0a) equal to zero, we have

$$(1-w)\frac{\eta|h_2|^2}{1+NP\eta|h_2|^2} + w\frac{|h_1|^2}{1+P|h_1|^2} = \lambda\ln 2. \tag{34}$$

Based on above, the optimal P given λ and $\mathbf{v}$ is either equal to zero or determined by solving equation (34). ■

IV. PARASITIC SETUP

In this section, we investigate the ergodic weighted-sum-rate maximization problem for the parasitic setup. We first analyze the instantaneous achievable rate and then investigates the resource allocation policy.

A. INSTANTANEOUS ACHIEVABLE RATE ANALYSIS

Since s_n and c_n have the same symbol duration, the primary transmission and BD transmission interfere with each other, which is different from the $N \gg 1$ case. The received signal is expressed as follows

$$y_n = \sqrt{P}h_1 s_n + \sqrt{P\alpha\eta}h_2 s_n c_n + u_n. \tag{35}$$

We introduce the SIC technique to decode c_n and s_n. The strong primary signal s_n is decoded firstly, meanwhile the backscatter signal $s_n c_n$ is treated as interference. Thus the signal-to-interference-plus-noise ratio (SINR) for decoding s_n is

$$\gamma_{\rm s} = \frac{P|h_1|^2}{1 + P\alpha\eta|h_2|^2}. \tag{36}$$

However, the distribution of $s_n c_n$ is a very complicated. To facilitate our analysis, we suggest a lower bound for the achievable rate of the primary system by approximating $s_n c_n$ as CSCG distribution, since the CSCG distributed interference is the worst case [33, Th. 7.2.5]. Then, the achievable rate of the primary system can be approximated as

$$\begin{aligned} R_{\rm s} &\approx \log_2(1 + \gamma_{\rm s}\Gamma_{\rm s}) \\ &= \log_2(1 + \frac{\Gamma_{\rm s} P|h_1|^2}{1 + P\alpha\eta|h_2|^2}). \end{aligned} \tag{37}$$

After s_n is decoded, we remove the first additive interference term in (35), and the received signal becomes

$$y_n = \sqrt{P\alpha\eta}h_2 s_n c_n + u_n. \tag{38}$$

The instantaneous SNR for decoding c_n given s_n is

$$\gamma_{c|s} = P\alpha\eta\,|h_2 s_n|^2\,. \tag{39}$$

As s_n follows CSCG distribution, $|s_n|^2$ follows standard exponential distribution, and the achievable rate of BD transmission is

$$\begin{aligned} R_{\rm c} &= \mathbb{E}_{|s_n|^2}\left[\log_2(1 + \gamma_{c|s}\Gamma_{\rm c}\right] \\ &= \int_0^\infty \log_2(1 + \Gamma_{\rm c} P\alpha\eta\,|h_2|^2 x)e^{-x}{\rm d}x \\ &= -e^{\frac{1}{\Gamma_{\rm c} P\alpha\eta|h_2|^2}}\,{\rm Ei}(-\frac{1}{\Gamma_{\rm c} P\alpha\eta\,|h_2|^2})\log_2 e. \end{aligned} \tag{40}$$

The instantaneous transmit power P and the reflection coefficient α in the achievable rate expressions shown in (37) and (40) are coupled to each other. We introduce two new variables $p = P$ and $q = \alpha P$. According to (7) and (8), p and q should satisfy:

$$p(\mathbf{v}) \geq 0, \quad \forall \mathbf{v}, \tag{41}$$

$$0 \leq q(\mathbf{v}) \leq p(\mathbf{v}), \quad \forall \mathbf{v}. \tag{42}$$

Then, substituting $\Gamma_{\rm s} = \Gamma_{\rm c} = 1$, $p = P$ and $q = \alpha P$ into (37) and (40), we have

$$R_{\rm s} = \log_2(1 + \frac{p|h_1|^2}{1 + q\eta|h_2|^2}), \tag{43}$$

$$R_{\rm c} = -e^{\frac{1}{q\eta|h_2|^2}}\,{\rm Ei}(-\frac{1}{q\eta\,|h_2|^2})\log_2 e. \tag{44}$$

Remark: When BD is shut down, the primary data rate is $\tilde{R}_{\rm s} = \log_2(1 + P|h_1|^2)$. However, from (43) and (44), if we want to achieve backscatter transmission, i.e., $R_{\rm c} > 0$, the primary transmission is interfered by the backscatter signal, and we have $R_{\rm s} < \tilde{R}_{\rm s}$. That is the reason why this setup is referred to as "parasitic".

B. RESOURCE ALLOCATION UNDER ST POWER CONSTRAINT

Substituting p into (9), the ST power constraint becomes

$$p(\mathbf{v}) \leq P_{\rm ST}, \ \forall \mathbf{v}. \tag{45}$$

Then the ergodic weighted-sum-rate maximization problem is expressed as

$$\begin{aligned} (\text{P1}) \ \max_{p(\mathbf{v}),q(\mathbf{v})} \quad & \mathbb{E}[(1-w)R_{\rm s} + wR_{\rm c}] \\ \mathbf{s.t.}\ & (41),\ (42),\ (45). \end{aligned}$$

From (43) and (44), $R_{\rm c}$ is the concave function of q. However, $R_{\rm c}$ is the convex function of q. Therefore, (P1) is non-convex problem, and the conventional convex optimization techniques cannot be applied to solve (P1).

The main idea of our proposed algorithm to solve (P1) is that: first, we decompose the original problem into individual subproblems over different fading states by considering all the constraints are short term, and then each subproblem is solved by employing the concave-convex procedure based on the difference-of-convex structure of the objective function.

1) DECOMPOSE THE ORIGINAL PROBLEM OVER DIFFERENT FADING STATES

In (P1), all the constraints (41), (42) and (45) are short term. Therefore, the original problem can be decomposed into individual subproblems over different fading states. For a particular fading state h_1 and h_2, the associated subproblem can be shown to be

$$\begin{aligned} (\text{P1a}) \ \max_{p,q} \ & Q_1(p,q) \\ \mathbf{s.t.}\ & 0 \leq p \leq P_{\rm ST}, \\ & 0 \leq q \leq p, \end{aligned}$$

where the objective function is

$$\begin{aligned} Q_1(p,q) &= (1-w)R_{\rm s} + wR_{\rm c} \\ &= (1-w)\log_2(1 + \frac{p|h_1|^2}{1 + q\eta|h_2|^2}) \\ &\quad - we^{\frac{1}{q\eta|h_2|^2}}\,{\rm Ei}(-\frac{1}{q\eta\,|h_2|^2})\log_2 e. \end{aligned} \tag{46}$$

Obviously, $Q_1(p, q)$ is the increasing function of p. Therefore, we have the optimal p:

$$p^\star = P_{\mathrm{ST}}. \tag{47}$$

Then, (P1a) is transformed to

$$\begin{aligned}(\text{P1b}) \ \max_{q} \ & \hat{Q}_1(q) \\ \mathbf{s.t.}\ & 0 \le q \le p^\star,\end{aligned}$$

where $\hat{Q}_1(q) = Q_1(p^\star, q)$.

2) REPRESENT $\hat{Q}_1(q)$ AS THE DIFFERENCE-OF-CONVEX STRUCTURE

Since $\hat{Q}_1(q)$ is non-convex function, (P1b) is still non-convex problem. To solve (P1b), we define two auxiliary functions as follows

$$H_1(q) = (w-1)\log_2(1+q\eta|h_2|^2), \tag{48}$$

$$\begin{aligned}D_1(q) = {} & (1-w)\log_2(1+p^\star|h_1|^2+q\eta|h_2|^2) \\ & - we^{\frac{1}{q\eta|h_2|^2}}\mathrm{Ei}(-\frac{1}{q\eta\,|h_2|^2})\log_2 e.\end{aligned} \tag{49}$$

Then, $\hat{Q}_1(q)$ can be written as

$$\hat{Q}_1(q) = H_1(q) + D_1(q). \tag{50}$$

Since $0 \le w \le 1$, $H_1(q)$ is convex, and $D_1(q)$ is concave. Therefore, the objective function of problem (P1b) has a difference-of-convex structure, and problem (P1b) can be efficiently solved by the concave-convex procedure [34].

3) ADOPTING THE CONCAVE-CONVEX PROCEDURE

The main idea of the concave-convex procedure is to transform problem (P1b) into a sequence of convex optimization problems by linearizing the convex part $H_1(q)$.

Denote $q^{(i)}$ as the fixed point at the i-th iteration. Then (P1b) can be solved by the following sequence programming

$$\begin{aligned}q^{(i+1)} = {} & \arg\max_{q} \bar{Q}_1(q) \\ & \mathbf{s.t.}\ 0 \le q \le p^\star,\end{aligned}$$

where

$$\bar{Q}_1(q) = D_1(q) + qH_1'(q^{(i)}), \tag{51}$$

and $H_1'(q) = \frac{(w-1)\eta|h_2|^2}{1+q\eta|h_2|^2}\log_2 e$ is the first-order derivative of $H_1(q)$. Denote $a^{(i)} = H_1'(q^{(i)})$. $\bar{Q}_1(q)$ can be written as

$$\bar{Q}_1(q) = D_1(q) + a^{(i)}q. \tag{52}$$

Theorem 3: The optimal solution for above optimization problem is

$$q^{(i+1)} = \begin{cases} 0, & \bar{q} < 0 \\ \bar{q}, & 0 \le \bar{q} \le p^\star \\ p^\star, & \bar{q} > p^\star \end{cases} \tag{53}$$

where $\bar{q}$ satisfies $\bar{Q}_1'(\bar{q}) = 0$.

Proof: The proof is straightforward, and thus is omitted here for brevity. ∎

Algorithm 1 The Concave-Convex Procedure for Solving (P1b)

Input: channel coefficients h_1 and h_2, ST power constraint P_{ST}.

1: Initialize $q^{(0)} = P_{\mathrm{ST}}$ and small threshold constant $\epsilon = 10^{-4}$. Let $i = 0$.
Repeat
2: Update $q^{(i+1)}$ according to (53).
3: Update iteration index $i = i + 1$.
Until $\left(\hat{Q}_1(q^{(i)}) - \hat{Q}_1(q^{(i-1)})\right) < \epsilon$.

Output: $q^\star = q^{(i)}$.

The remaining task is to obtain $\bar{q}$, and we have the following proposition.

Proposition 2: $\bar{Q}_1'(q)$ is monotonically decreasing function of q, so $\bar{q}$ can be obtained via bisearch algorithm efficiently.

Proof: See Appendix B. ∎

We summarize the above concave-convex procedure for solving (P1b) in **Algorithm 1**.

C. RESOURCE ALLOCATION UNDER LT POWER CONSTRAINT

Substituting $p = P$ into (10), the LT power constraint becomes

$$\mathbb{E}[p(\mathbf{v})] \le P_{\mathrm{LT}}. \tag{54}$$

Then we have optimization problem:

$$\begin{aligned}(\text{P2}) \ \max_{p(\mathbf{v}),q(\mathbf{v})} \ & Q_2\left(p(\mathbf{v}), q(\mathbf{v})\right) \triangleq \mathbb{E}[(1-w)R_{\mathrm{s}} + wR_{\mathrm{c}}] \\ \mathbf{s.t.}\ & (41),\ (42),\ (54).\end{aligned}$$

Although the feasible set of (P2) is convex, the objective function is non-convex. Therefore, (P2) is non-convex problem which is challenging to be solved.

The main idea of our proposed algorithm to solve (P2) is a little different from the approach employed for (P1). Due to the long-term power constraint, (P2) cannot be decomposed into individual subproblems and solved directly. Instead, we first transform (P2) into a sequence of convex problems based on the concave-convex procedure. Then, the long-term power constraint is tackled by the Lagrange dual variable. Since all the constrains are short-term now, the optimization problem is decomposed into individual subproblems. Finally, these convex subproblems are solved for each fading state.

1) REPRESENT $Q_2\left(p(\mathbf{v}), q(\mathbf{v})\right)$ AS THE DIFFERENCE-OF-CONVEX STRUCTURE

To solve (P2), we define two auxiliary functions as follows

$$\begin{aligned}D_2\left(p(\mathbf{v}), q(\mathbf{v})\right) = {} & \mathbb{E}\Big[(1-w)\log_2(1+p|h_1|^2+q\eta|h_2|^2) \\ & - we^{\frac{1}{q\eta|h_2|^2}}\mathrm{Ei}(-\frac{1}{q\eta\,|h_2|^2})\log_2 e\Big],\end{aligned} \tag{55}$$

$$H_2\left(q(\mathbf{v})\right) = (w-1)\mathbb{E}\left[\log_2(1+q\eta|h_2|^2)\right]. \tag{56}$$

$H_2\left(q(\mathbf{v})\right)$ in (56) is convex, and $D_2\left(p(\mathbf{v}), q(\mathbf{v})\right)$ in (55) is concave. Then $Q_2\left(p(\mathbf{v}), q(\mathbf{v})\right)$ can be represented as the difference-of-convex structure

$$Q_2\left(p(\mathbf{v}), q(\mathbf{v})\right) = D_2\left(p(\mathbf{v}), q(\mathbf{v})\right) + H_2\left(q(\mathbf{v})\right), \tag{57}$$

and we can solve (P2) via the concave-convex procedure.

2) ADOPTING THE CONCAVE-CONVEX PROCEDURE

Denote $\left[p^{(i)}(\mathbf{v}), q^{(i)}(\mathbf{v})\right]$ as the initial resource allocation policy at the i-th iteration. Then (P2) can be solved by the following sequence programming

$$\begin{aligned}(\mathrm{P2}-i): &\left[p^{(i+1)}(\mathbf{v}), q^{(i+1)}(\mathbf{v})\right] \\ &= \arg\max_{p(\mathbf{v}),q(\mathbf{v})} \hat{Q}_2\left(p(\mathbf{v}), q(\mathbf{v})\right) \\ &\quad \mathbf{s.t.}\ p(\mathbf{v}) \geq 0, \quad \forall \mathbf{v} && \text{(58a)} \\ &\quad 0 \leq q(\mathbf{v}) \leq p(\mathbf{v}), \quad \forall \mathbf{v} && \text{(58b)} \\ &\quad \mathbb{E}[p(\mathbf{v})] \leq P_{\mathrm{LT}}, && \text{(58c)}\end{aligned}$$

where

$$\begin{aligned}&\hat{Q}_2\left(p(\mathbf{v}), q(\mathbf{v})\right) \\ &= D_2\left(p(\mathbf{v}), q(\mathbf{v})\right) + \mathbb{E}_{\mathbf{v}}\left[q(\mathbf{v})H_2'\left(q^{(i)}(\mathbf{v})\right)\right] \\ &= D_2\left(p(\mathbf{v}), q(\mathbf{v})\right) + \frac{w-1}{\ln 2}\mathbb{E}_{\mathbf{v}}\left[\frac{\eta|h_2|^2 q(\mathbf{v})}{1+q^{(i)}(\mathbf{v})\eta|h_2|^2}\right]. \end{aligned} \tag{59}$$

Apparently, (P2-i) is convex optimization problem, and can be solved by using Lagrange dual decomposition.

3) SOLVE (P2-i) BY DUAL DECOMPOSITION

It is noted that in (P2-i), only the power constraint in (58c) is LT while all the other constraints are ST. We introduce the Lagrange dual variable λ ($\lambda \geq 0$) associated with the LT power constraint. The Lagrangian of (P2-i) can be written as

$$\mathcal{L}\big(p(\mathbf{v}), q(\mathbf{v}), \lambda\big) = \hat{Q}_2\big(p(\mathbf{v}), q(\mathbf{v})\big) - \lambda\big(\mathbb{E}_{\mathbf{v}}[p(\mathbf{v})] - P_{\mathrm{LT}}\big). \tag{60}$$

Then the Lagrangian dual function is given by

$$\begin{aligned}\mathcal{G}(\lambda) = &\max_{p(\mathbf{v}),q(\mathbf{v})} \mathcal{L}\big(p(\mathbf{v}), q(\mathbf{v}), \lambda\big) \\ &\mathbf{s.t.}\ (58a),\ (58b),\end{aligned}$$

and the dual problem is accordingly defined as

$$(\mathrm{P2}-i')\ \min_{\lambda\geq 0}\ \mathcal{G}(\lambda). \tag{61}$$

It can be verified that the duality gap is zero, and thus solving (P2-i') is equivalent to solving the original problem (P2-i).

Next, we focus on obtaining $\mathcal{G}(\lambda)$ with some given λ. After $\mathcal{G}(\lambda)$ is obtained for all the fading states, the minimization of $\mathcal{G}(\lambda)$ in (P2-i') can be resolved efficiently via the ellipsoid method [35], of which we omit the details here for brevity.

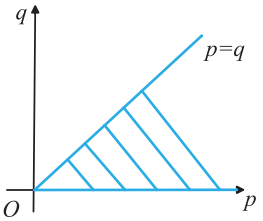

Fig. 5. Illustration of the feasible region of (P3).

4) DECOMPOSE (P2-i') OVER DIFFERENT FADING STATES

Proposition 3: The dual function $\mathcal{G}(\lambda)$ can be obtained by solving following subproblem for particular fading state:

$$\begin{aligned}(\mathrm{P3})\ &\max_{p,q}\ Q_3(p,q) \triangleq \bar{D}_2(p,q) + H_3(q) - \lambda p \\ &\mathbf{s.t.}\ p \geq 0, \\ &\quad 0 \leq q \leq p,\end{aligned}$$

where

$$\begin{aligned}\bar{D}_2(p,q) = &(1-w)\log_2(1+p|h_1|^2+q\eta|h_2|^2) \\ &- we^{\frac{1}{q\eta|h_2|^2}} Ei\left(-\frac{1}{q\eta\,|h_2|^2}\right)\log_2 e, \end{aligned} \tag{62}$$

$$H_3(q) = (w-1)\frac{\eta|h_2|^2 q}{1+q^{(i)}\eta|h_2|^2}\log_2 e. \tag{63}$$

Proof: See Appendix C. ■

5) SOLVE (P3) FOR PARTICULAR FADING STATE

(P3) is convex, but it does not have a closed-form solution due to the exponential integral in $\bar{D}_2(p,q)$. The feasible region of (P3) is illustrated in Fig. 5 according to the constraints $p \geq 0$ and $0 \leq q \leq p$. Then, we have the following proposition.

Proposition 4: Suppose $[\hat{p}, \hat{q}]$ is the solution to the following unconstrained optimization problem:

$$\hat{p}, \hat{q} = \arg\max_{p,q}\ Q_3(p,q), \tag{64}$$

$[\hat{p}, \hat{q}]$ is the solution to (P3) if point $[\hat{p}, \hat{q}]$ is located in the feasible region. Otherwise, the solution to (P3) should be located on the boundaries of the feasible region.

Proof: The proof is straightforward based on the convex optimization theory [32], and thus is omitted here. ■

Based on *Proposition* 4, a two-step approach to solve (P3) is presented as follows.

Step I: *Solving the unconstrained optimization problem*

$$\hat{p}, \hat{q} = \arg\max_{p,q}\ Q_3(p,q) \triangleq \bar{D}_2(p,q) + H_3(q) - \lambda p. \tag{65}$$

From (63), we have

$$\frac{\partial H_3(q)}{\partial q} = (w-1)\frac{\eta|h_2|^2}{1+q^{(i)}\eta|h_2|^2}\log_2 e, \tag{66}$$

which is irrelevant to q. Then, $\hat{p}$ and $\hat{q}$ is given in the following theorem.

Theorem 4: $\hat{q}$ *can be obtained by solving following equation:*

$$\left.\frac{\partial \bar{D}_2(p,q)}{\partial q}\right|_{q=\hat{q}} = (1-w)\frac{\eta|h_2|^2}{1+q^{(i)}\eta|h_2|^2}\log_2 e. \quad (67)$$

Then $\hat{p}$ *can be obtained via following expression:*

$$\hat{p} = \frac{1}{|h_1|^2}\left(\frac{1}{\lambda}(1-w)|h_1|^2\log_2 e - \hat{q}\eta|h_2|^2 - 1\right). \quad (68)$$

Proof: See Appendix D. ∎

From (62), we have

$$\frac{\partial \bar{D}_2(p,q)}{\partial q} = \frac{(1-w)\eta|h_2|^2}{(1+p|h_1|^2+q\eta|h_2|^2)\ln 2} + \frac{w}{\eta|h_2|^2q^2\ln 2}\left[e^{\frac{1}{\eta|h_2|^2q}}\mathrm{Ei}(-\frac{1}{\eta|h_2|^2q}) + \eta|h_2|^2q\right]. \quad (69)$$

Substituting (68) into (69), $\frac{\partial \bar{D}_2(p,q)}{\partial q}$ can be written as

$$\frac{\partial \bar{D}_2(p,q)}{\partial q} = \frac{\lambda|h_2|^2}{h_1^2} + \frac{w}{q\ln 2} + \frac{w}{\eta|h_2|^2q^2\ln 2}e^{\frac{1}{\eta|h_2|^2q}}\mathrm{Ei}(-\frac{1}{\eta|h_2|^2q}). \quad (70)$$

$\frac{\partial \bar{D}_2(p,q)}{\partial q}$ in (70) is monotonic decreasing function of q. Thus, equation (67) can be efficiently solved via the bisearch algorithm.

Step II: Checking the feasible region.

From *Proposition* 4, if $[\hat{p},\hat{q}]$ is located in the feasible region, the optimal solutions for (P3) is

$$p^\star = \hat{p}, \quad (71)$$
$$q^\star = \hat{q}. \quad (72)$$

Otherwise, $p^\star$ and $q^\star$ should be obtained on the feasible region boundaries. From Fig. 5, there are two cases to be discussed.

- *Boundary* $q = 0$ and $p \geq 0$:
  In this case, we have
  $$Q_3(p,0) = \bar{D}_2(p,0) + H_3(0) - \lambda p = (1-w)\log_2(1+p|h_1|^2) - \lambda p. \quad (73)$$
  By solving $\max_{p\geq 0} Q_3(p,0)$, we have
  $$\hat{p}_1 = \left(\frac{1}{|h_1|^2}\left(\frac{(1-w)|h_1|^2}{\lambda\ln 2} - 1\right)\right)^+. \quad (74)$$
- *Boundary* $q = p$ and $p > 0$:
  In this case, we have
  $$Q_3(p,p) = \bar{D}_2(p,p) + H_3(p) - \lambda p, \quad (75)$$
  and we need to solve $\max_{p\geq 0} Q_3(p,p)$. From (62), we have
  $$\frac{\partial \bar{D}_2(p,p)}{\partial p} = \frac{(1-w)\left(|h_1|^2+\eta|h_2|^2\right)}{\left(1+p\left(|h_1|^2+\eta|h_2|^2\right)\right)\ln 2} + \frac{w}{\eta|h_2|^2p^2\ln 2}\left[e^{\frac{1}{\eta|h_2|^2p}}\mathrm{Ei}(-\frac{1}{\eta|h_2|^2p}) + \eta|h_2|^2p\right], \quad (76)$$
  which is monotonic decreasing function of p. Then the first-order derivative of $Q_3(p,p)$ is
  $$\frac{\partial Q_3(p,p)}{\partial p} = \frac{\partial \bar{D}_2(p,p)}{\partial p} + \left.\frac{\partial H_3(q)}{\partial q}\right|_{q=p} - \lambda, \quad (77)$$
  where $\frac{\partial H_3(q)}{\partial q}$ is shown in (66) which is a constant. Therefore, $\frac{\partial Q_3(p,p)}{\partial p}$ is also monotonic decreasing function of p. Suppose $\hat{p}_2$ satisfies $\left.\frac{\partial Q_3(p,p)}{\partial p}\right|_{p=\hat{p}_2} = 0$. $\hat{p}_2$ is the solution of $\max_{p>0} Q_3(p,p)$, which can be solved efficiently via the bisearch algorithm.

In the end, if $Q_3(\hat{p}_1,0) \geq Q_3(\hat{p}_2,\hat{p}_2)$, we have $p^\star = \hat{p}_1$ and $q^\star = 0$; otherwise, we have $p^\star = \hat{p}_2$ and $q^\star = \hat{p}_2$.

We summarize the above concave-convex procedure based algorithm for (P2) in **Algorithm 2**.

Algorithm 2 The Concave-Convex Procedure for Solving (P2)

Input: channel coefficients h_1 and h_2 for each fading state, LT power constraint P_{LT}.

1: Initialize the resource allocation policy with $p^{(0)}(\mathbf{v}) = q^{(0)}(\mathbf{v}) = P_{\mathrm{LT}}$. The threshold constant is set as $\epsilon = 10^{-4}$. Let $i = 0$.
   Repeat
2: Transform (P2) into (P2-i) using $p^{(i)}(\mathbf{v})$ and $q^{(i)}(\mathbf{v})$.
3: Initialize the Lagrange dual variable $\lambda = \lambda_0$ and $j = 0$;
   Repeat
4: Solve (P3) for all the fading states given λ.
5: Update iteration index j = j + 1.
6: Update $\lambda = \lambda_j$ via the sub-gradient method.
   Until $\left|\mathcal{G}(\lambda_j) - \mathcal{G}(\lambda_{j-1})\right| < \epsilon$.
7: Update $p^{(i+1)}(\mathbf{v})$ and $q^{(i+1)}(\mathbf{v})$ according to the solutions of (P2-i).
8: Update iteration index $i = i + 1$.
   Until $Q_2\left(p^{(i)}(\mathbf{v}), q^{(i)}(\mathbf{v})\right) - Q_2\left(p^{(i-1)}(\mathbf{v}), q^{(i-1)}(\mathbf{v})\right) < \epsilon$.

Output: $p(\mathbf{v}) = p^{(i)}(\mathbf{v})$ and $q(\mathbf{v}) = q^{(i)}(\mathbf{v})$.

V. NUMERICAL RESULTS

In this section, several numerical examples are presented to evaluate the achievable rates of both the primary transmission and backscatter transmission with the proposed resource allocation strategies. All the channels involved are assumed to be Rayleigh fading, and the channel power gains are exponentially distributed. It is noted that this assumption does not affect the structure of the problem studied and the solution obtained. For ease of notation, the ergodic rates for primary and BD transmissions are denoted by R_{s} and R_{c}, respectively, in this section. In addition, all the simulation results are obtained by averaging over 10^5 channel realizations.

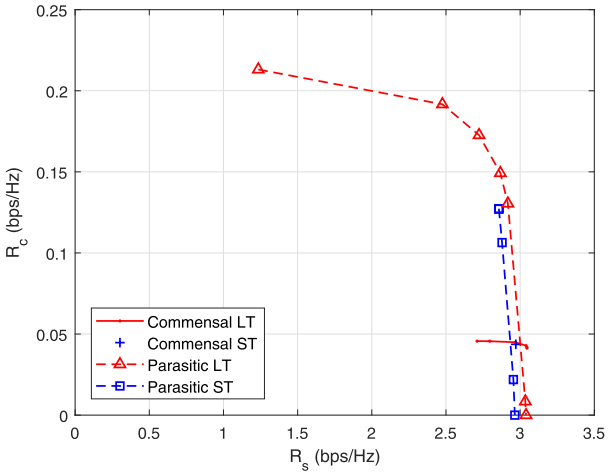

Fig. 6. Achievable rate tradeoff when $P_{ST} = 10$ dB, $P_{LT} = 10$ dB, $\eta = -20$ dB and $N = 50$.

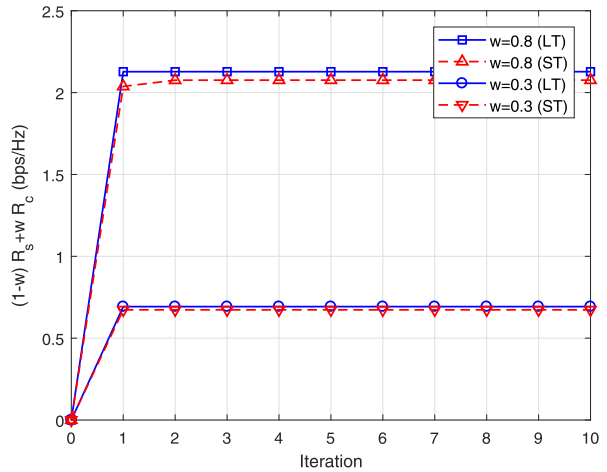

Fig. 7. Convergence behavior of the proposed algorithm for the parasitic setup using the same simulation conditions of Fig. 6.

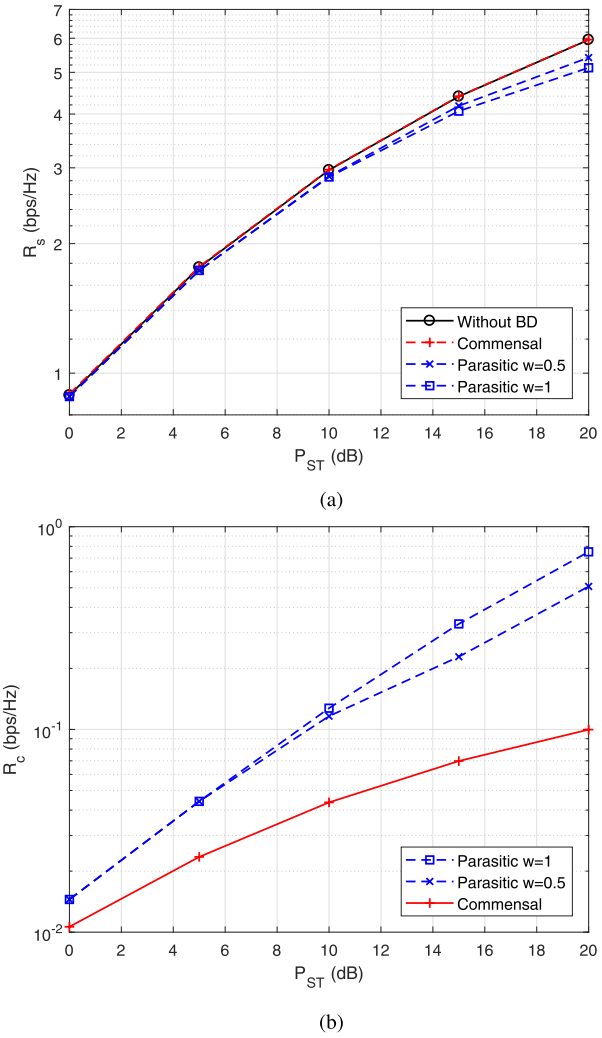

Fig. 8. The achievable rates vs ST power constraint P_{ST} when $\eta = -20$ dB and $N = 50$. (a) Primary transmission. (b) Backscatter transmission.

A. RATE REGION AND CONVERGENCE BEHAVIOR ANALYSIS

Fig. 6 shows the ergodic achievable rate tradeoff between the primary and backscatter transmissions in the symbiotic radio system by increasing w from 0 to 1, in which $P_{\mathrm{ST}} = 10$ dB, $P_{\mathrm{LT}} = 10$ dB, $\eta = -20$ dB and $N = 50$. Since w is the weighting factor for R_{c}, a larger value of w will render a higher R_{c}. Also, it is shown that, in all curves, R_{s} decreases with the increase of R_{c}. Hence, it is impossible to improve both R_{s} and R_{c} simultaneously, even for the commensal setup. In addition, we observe that the dynamic range of R_{c} for the commensal setup is much smaller than that for the parasitic setup. This is because, to increase R_{c}, only the transmit power can be adjusted for the commensal setup. However, both the transmit power and reflection coefficient are optimized for the parasitic setup.

It is worth noting that, we have derived the optimal resource allocation policy for the commensal setup. For the parasitic setup, however, due to the non-convex structure of the problem in (P1) and (P2), only suboptimal solutions can be obtained by using the proposed algorithm. To evaluate the convergence speed of the proposed algorithm, we present Fig. 7 for the parasitic setup under the same simulation conditions of Fig. 6. It can be observed that the algorithm converges within 3 iterations. Meanwhile, since all the sub-problems in every iteration are convex, the time complexity of the proposed algorithm is polynomial. In practice, for the symbiotic radio system, a look-up table for the resource allocation policy can be pre-stored for different channel realizations, and the look-up table needs to be updated only when the large-scale fading changes sufficiently.

B. IMPACT OF TRANSMIT POWER CONSTRAINTS

The achievable rates of the primary transmission and backscatter transmission with respect to the ST power constraints are illustrated in Fig. 8(a) and Fig. 8(b), respectively, for $\eta = -20$ dB and $N = 50$. To evaluate the impact of BD on R_{s}, we provide a baseline for the pure primary system cases, i.e., when BD transmission is shut down, in Fig. 8(a).

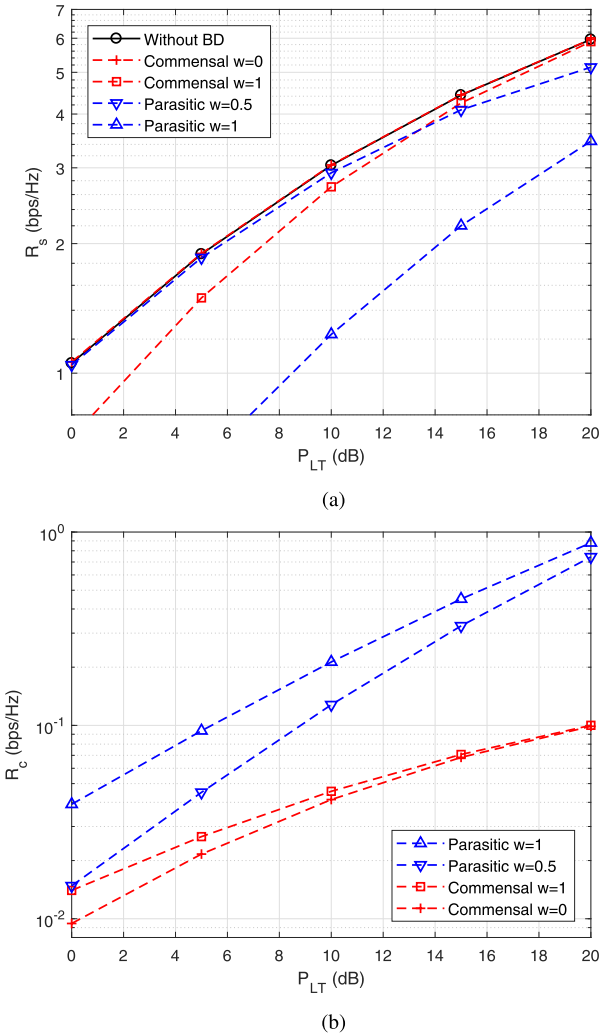

Fig. 9. The achievable rates vs LT power constraint P_{LT} when $\eta = -20$ dB and $N = 50$. (a) Primary transmission. (b) Backscatter transmission.

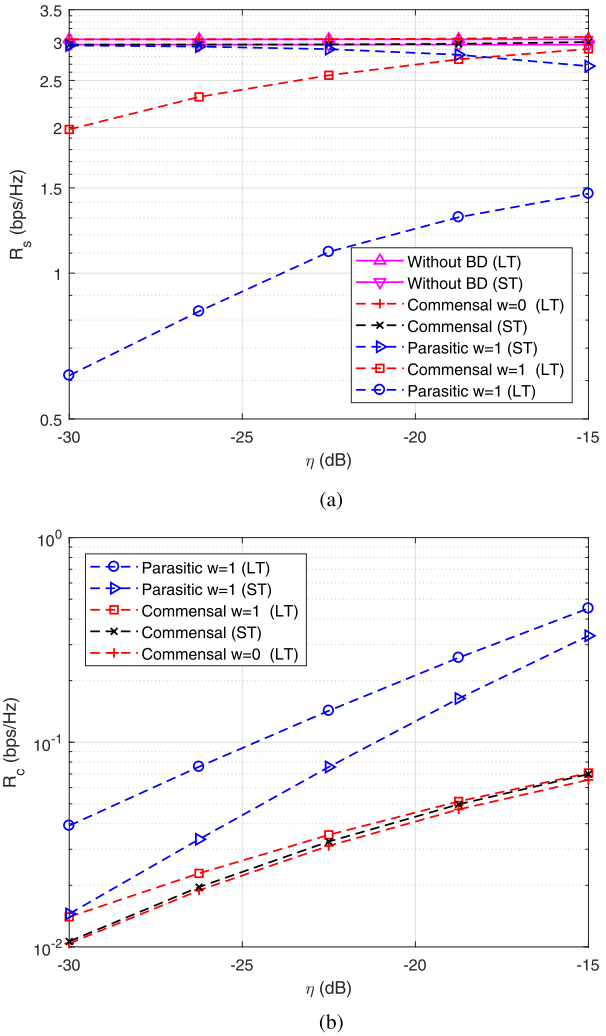

Fig. 10. The achievable rates vs the backscatter loss η when $P_{\mathrm{ST}} = 10$ dB, $P_{\mathrm{LT}} = 10$ dB and $N = 50$. (a) Primary transmission. (b) Backscatter transmission.

As expected, for the commensal setup, the achieved R_{s} is slightly better than the baseline, since the backscatter link provides an additional beneficial signal path for primary transmission. Meanwhile, for the parasitic setup, R_{s} is lower than the baseline, since the backscatter transmission interferes the primary transmission. Comparing Fig. 8(a) and Fig. 8(b), we can see that the parasitic setup may achieve higher R_{c} than the commensal setup with a slight performance degradation of R_{s}, when a proper w is chosen. For example, by setting $w = 0.5$, R_{c} for the parasitic setup increases more than 4 times than that for the commensal setup, while R_{s} decreases less than 10%.

Fig. 9 illustrates the achievable rates of the two transmissions with respect to the LT power constraints for $\eta = -20$ dB and $N = 50$. For the commensal setup, we consider $w = 0$ and $w = 1$ for resource allocation which focus on R_{s} and R_{c}, respectively. For the parasitic setup, $w = 0.5$ and $w = 1$ are considered, and in this setup, BD is shut down when $w = 0$. It is seen that, the performance gap between the curves for different weights decreases as the increase of P_{LT}. This is because, the water-pouring gain from resource allocation over different fading states becomes smaller for high SNR region [36]. Besides, by comparing the two figures, we also observe that a higher R_{c} renders a lower R_{s}, which is consistent with the observations in Fig. 6 and Fig. 8. In addition, the parasitic setup with $w = 0.5$ performs quite well, which achieves a high R_{c} with only a slight loss of R_{s}.

C. IMPACT OF BACKSCATTER LOSS FACTOR

Finally, Fig. 10 illustrates the impact of η on the achievable rates for both ST and LT power constraints when $P_{\mathrm{ST}} = 10$ dB, $P_{\mathrm{LT}} = 10$ dB and $N = 50$. It is seen from Fig. 10(a) that, R_{s} in commensal setup increases as η increases. This coincides with our proposition that the backscatter signal provides a beneficial signal path for the primary transmission. However, for the parasitic setup, different phenomenon is observed when $w = 1$. Under ST power constraint, we can

see that R_s decreases as η increases. This is because, for this case, the optimal solution is $\alpha = 1$ and $P = P_{ST}$, and a stronger backscatter signal results in stronger interference to the primary transmission. On the other hand, R_s increases as η increases under LT power constraint. We conjecture that, in this case, the objective is to maximize R_c, and higher transmit power will be allocated to the fading state with higher backscatter channel power gain. As a result, R_s may not necessarily decrease, since the transmit power and the strength of interference both increase. These simulation results imply that, even for the parasitic setup, the enhancement of the backscatter signal may also benefit the primary transmission using the proposed power allocation strategy. In Fig. 10(b), it is seen that, when η increases, R_c increases for all the simulated cases as the backscatter link becomes stronger. We also observe that, the parasitic setup with $w = 1$ achieves higher R_c than the commensal setup.

VI. CONCLUSION

In this paper, we investigate the resource allocation problems for symbiotic radio system when the channel fading is considered. Two practical transmission setups are proposed to overcome the spectrum growth phenomenon. One is the commensal setup, and the other is the parasitic setup. Then, the ergodic weighted sum rate of the primary and backscatter transmissions is maximized by jointly optimizing the transmit power of the primary transmitter and the reflection coefficient of the backscatter device. Both short-term and long-term transmit-power constraints are considered. Optimal solutions for the commensal setup are derived via standard convex optimization procedure. Suboptimal solutions of the non-convex optimization problem for the parasitic setup are derived via the concave-convex procedure. Simulation results have been given to evaluate the performance of the proposed resource allocation policies for different scenarios.

APPENDIX A
PROOF OF PROPOSITION 1

From (16), R_s can be written as

$$\begin{aligned} R_s &= \int_0^\infty \log_2(1+Px) f_{\kappa_1}(x)\,\mathrm{d}x \\ &= \log_2(1+P|h_1|^2) + \int_0^\infty \log_2\left(\frac{1+Px}{1+P|h_1|^2}\right) f_{\kappa_1}(x)\,\mathrm{d}x. \end{aligned} \tag{78}$$

Denote $Z = \int_0^\infty \log_2\left(\frac{1+Px}{1+P|h_1|^2}\right) f_{\kappa_1}(x)\,\mathrm{d}x$. When P approaches to infinity, we have

$$\begin{aligned} Z &= \int_0^\infty \log_2\left(\frac{1}{1+P|h_1|^2} + \frac{Px}{1+P|h_1|^2}\right) f_{\kappa_1}(x)\,\mathrm{d}x \\ &\approx \int_0^\infty \log_2\left(\frac{x}{|h_1|^2}\right) f_{\kappa_1}(x)\,\mathrm{d}x. \end{aligned} \tag{79}$$

From (15), $f_{\kappa_1}(x) = \frac{1}{\alpha\eta|h_2|^2} e^{-\frac{|h_1|^2+x}{\alpha\eta|h_2|^2}} I_0\left(\frac{2|h_1|}{\alpha\eta|h_2|^2}\sqrt{x}\right)$. Let $\theta = \frac{\kappa_1}{\alpha\eta|h_2|^2}$. The PDF of θ is

$$f_\theta(x) = e^{-\left(\frac{|h_1|^2}{\alpha\eta|h_2|^2}+x\right)} I_0\left(2\sqrt{x\frac{|h_1|^2}{\alpha\eta|h_2|^2}}\right). \tag{80}$$

From [37], it is known that, supposing a random variable V following standard non-central chi-square distribution with 2-degree of freedom whose PDF is

$$f_V(x) = e^{-(\varepsilon^2+x)} I_0(2\varepsilon\sqrt{x}), \tag{81}$$

the expected value of the logarithm of V is

$$\mathbb{E}[\ln V] = \ln(\varepsilon^2) - \mathrm{Ei}(-\varepsilon^2). \tag{82}$$

Then, based on (81) and (82), we have

$$\mathbb{E}[\ln\theta] = \ln\left(\frac{|h_1|^2}{\alpha\eta|h_2|^2}\right) - \mathrm{Ei}\left(-\frac{|h_1|^2}{\alpha\eta|h_2|^2}\right). \tag{83}$$

Substituting $\theta = \frac{\kappa_1}{\alpha\eta|h_2|^2}$, (80) and (83), Z in (79) becomes:

$$\begin{aligned} Z &= \int_0^\infty \log_2\left(\frac{\alpha\eta|h_2|^2 x}{|h_1|^2}\right) f_\theta(x)\,\mathrm{d}x \\ &= \log_2\left(\frac{\alpha\eta|h_2|^2}{|h_1|^2}\right) + \int_0^\infty \log_2(x) f_\theta(x)\,\mathrm{d}x \\ &= -\mathrm{Ei}\left(-\frac{|h_1|^2}{\alpha\eta|h_2|^2}\right)\log_2 e. \end{aligned} \tag{84}$$

Finally, substituting (84) into (78), we have

$$R_s \approx \log_2(1+P|h_1|^2) - \mathrm{Ei}\left(-\frac{|h_1|^2}{\alpha\eta|h_2|^2}\right)\log_2 e, \tag{85}$$

and *Proposition* 1 is thus proved.

APPENDIX B
PROOF OF PROPOSITION 2

From (49), we have $D_1(q) = (1-w)\log_2(1+p^\star|h_1|^2 + q\eta|h_2|^2) + wR_c$. Thus the first-order derivative of $D_1(q)$ is

$$D_1'(q) = \frac{(1-w)\eta|h_2|^2}{(1+p^\star|h_1|^2+q\eta|h_2|^2)\ln 2} + w\frac{\partial R_c}{\partial q}. \tag{86}$$

Then, the first-order derivative of $\bar{Q}_1(q)$ in (52) is

$$\begin{aligned} \bar{Q}_1'(q) &= D_1'(q) + a^{(i)} \\ &= \frac{(1-w)\eta|h_2|^2}{(1+p^\star|h_1|^2+q\eta|h_2|^2)\ln 2} + w\frac{\partial R_c}{\partial q} + a^{(i)}. \end{aligned} \tag{87}$$

Apparently, the first term in (87) is monotonically decreasing function of q. Next, we focus on the second term.

From (40) and (44), the first-order derivative of R_c with respect to q can be represented in a closed-form by using $\int_0^\infty \frac{xe^{-\varrho x}}{x+1}\mathrm{d}x = e^{\varrho}\,\mathrm{Ei}(-\varrho) + \frac{1}{\varrho}$ [38, eq. (3.353.5)]:

$$\begin{aligned} \frac{\partial R_c}{\partial q} &= \int_0^\infty \frac{\eta\,|h_2|^2\,x\log_2 e}{1+q\eta\,|h_2|^2\,x} e^{-x}\mathrm{d}x \\ &= \frac{\log_2 e}{\eta|h_2|^2 q^2}\left[e^{\frac{1}{\eta|h_2|^2 q}}\mathrm{Ei}\left(-\frac{1}{\eta|h_2|^2 q}\right) + \eta|h_2|^2 q\right]. \end{aligned} \tag{88}$$

Hence, $\frac{\partial R_c}{\partial q}$ is also the monotonically decreasing function of q, and the proposition is proved.

APPENDIX C
PROOF OF PROPOSITION 3

From (60), $\mathcal{L}\big(p(\mathbf{v}), q(\mathbf{v}), \lambda\big)$ can be represented as

$$\mathcal{L}\big(p(\mathbf{v}), q(\mathbf{v}), \lambda\big) = \hat{Q}_2\big(p(\mathbf{v}), q(\mathbf{v})\big) - \lambda\mathbb{E}[p] + \lambda P_{\mathrm{LT}}. \quad (89)$$

Substituting (59) into (89), we have

$$\begin{aligned}\mathcal{L}\big(p(\mathbf{v}), q(\mathbf{v}), \lambda\big) &= D_2\left(p(\mathbf{v}), q(\mathbf{v})\right) \\ &\quad + \mathbb{E}\left[H_3\left(q\right) - \lambda p\right] + \lambda P_{\mathrm{LT}}. \quad (90)\end{aligned}$$

Then, substituting (55) into (90), we obtain

$$\begin{aligned}\mathcal{L}\big(p(\mathbf{v}), q(\mathbf{v}), \lambda\big) &= \mathbb{E}\Big[\bar{D}_2\left(p, q\right) + H_3\left(q\right) - \lambda p\Big] + \lambda P_{\mathrm{LT}} \\ &= \mathbb{E}\Big[Q_3\left(p, q\right)\Big] + \lambda P_{\mathrm{LT}}. \quad (91)\end{aligned}$$

Therefore, the dual function $\mathcal{G}(\lambda)$ can also be represented as

$$\begin{aligned}\mathcal{G}(\lambda) = \mathbb{E}\Big[\max_{p,q} Q_3\left(p, q\right)\Big] + \lambda P_{\mathrm{LT}} \\ \mathbf{s.t.}\ (58a),\ (58b).\end{aligned}$$

Since the constraints in (58a) and (58b) are short-term, the above $\mathcal{G}(\lambda)$ can be decomposed into individual subdual-functions for each fading state, and the proposition is proved.

APPENDIX D
PROOF OF THEOREM 4

Since $Q_3(p, q)$ is convex function, $\hat{p}$ and $\hat{q}$ should satisfy

$$\left.\frac{\partial Q_3(p, q)}{\partial p}\right|_{p=\hat{p}} = 0, \quad (92a)$$

$$\left.\frac{\partial Q_3(p, q)}{\partial q}\right|_{q=\hat{q}} = 0, \quad (92b)$$

respectively. The partial derivative of $Q_3(p, q)$ with respect to p is

$$\begin{aligned}\frac{\partial Q_3(p, q)}{\partial p} &= \frac{\partial \bar{D}_2(p, q)}{\partial p} - \lambda \\ &= (1-w)\frac{|h_1|^2}{1 + p|h_1|^2 + q\eta|h_2|^2}\log_2 e - \lambda. \quad (93)\end{aligned}$$

Substituting (93) into $\left.\frac{\partial Q_3(p,q)}{\partial p}\right|_{p=\hat{p}} = 0$, we have

$$\hat{p} = \frac{1}{|h_1|^2}\left(\frac{1}{\lambda}(1-w)|h_1|^2\log_2 e - \hat{q}\eta|h_2|^2 - 1\right). \quad (94)$$

Thus, equation (68) is proved.

In addition, the partial derivative of $Q_3(p, q)$ with respect to q is

$$\frac{\partial Q_3(p, q)}{\partial q} = \frac{\partial \bar{D}_2(p, q)}{\partial q} + \frac{\partial H_3(q)}{\partial q}. \quad (95)$$

Thus $\left.\frac{\partial Q_3(p,q)}{\partial q}\right|_{q=\hat{q}} = 0$ can be written as

$$\left.\frac{\partial \bar{D}_2(p, q)}{\partial q}\right|_{q=\hat{q}} = -\left.\frac{\partial H_3(q)}{\partial q}\right|_{q=\hat{q}}. \quad (96)$$

Substituting $\frac{\partial H_3(q)}{\partial q}$ in (66) into (96), equation (67) is obtained.

REFERENCES

[1] R. Long, H. Guo, G. Yang, Y.-C. Liang, and R. Zhang. (2018). "Symbiotic radio: A new communication paradigm for passive Internet-of-Things." [Online]. Available: https://arxiv.org/abs/1810.13068
[2] R. Long, H. Guo, L. Zhang, and Y.-C. Liang, "Full-duplex backscatter communications in symbiotic radio systems," *IEEE Access*, vol. 7, pp. 21597–21608, 2019.
[3] Q. Zhang, L. Zhang, Y.-C. Liang, and P. Y. Kam, "Backscatter-NOMA: A symbiotic system of cellular and Internet-of-Things networks," *IEEE Access*, vol. 7, pp. 20000–20013, 2019.
[4] M. L. Memon, N. Saxena, A. Roy, and D. R. Shin, "Backscatter communications: Inception of the battery-free era—A comprehensive survey," *Electron.*, vol. 8, no. 2, p. 129, 2019.
[5] C. Boyer and S. Roy, "Backscatter communication and RFID: Coding, energy, and MIMO analysis," *IEEE Trans. Commun.*, vol. 62, no. 3, pp. 770–785, Mar. 2014.
[6] J. D. Griffin and G. D. Durgin, "Complete link budgets for backscatter-radio and RFID systems," *IEEE Antennas Propag. Mag.*, vol. 51, no. 2, pp. 11–25, Apr. 2009.
[7] R. Duan, R. Jantti, H. Yiğitler, and K. Ruttik, "On the achievable rate of bistatic modulated rescatter systems," *IEEE Trans. Veh. Technol.*, vol. 66, no. 10, pp. 9609–9613, Oct. 2017.
[8] X. Kang, Y. C. Liang, and J. Yang, "Riding on the primary: A new spectrum sharing paradigm for wireless-powered IoT devices," *IEEE Trans. Wireless Commun.*, vol. 17, no. 9, pp. 6335–6347, Sep. 2018.
[9] L. Zhang, Y. C. Liang, and M. Xiao, "Spectrum sharing for Internet of Things: A survey," *IEEE Wireless Commun.*, to be published. doi: 10.1109/MWC.2018.1800259.
[10] L. Zhang, J. Liu, M. Xiao, G. Wu, Y.-C. Liang, and S. Li, "Performance analysis and optimization in downlink NOMA systems with cooperative full-duplex relaying," *IEEE J. Sel. Areas Commun.*, vol. 35, no. 10, pp. 2398–2412, Oct. 2017.
[11] X. Liu, Y. Gao, and F. Hu, "Optimal time scheduling scheme for wireless powered ambient backscatter communications in IoT networks," *IEEE Internet Things J.*, to be published. doi: 10.1109/JIOT.2018.2889700.
[12] N. V. Huynh, D. T. Hoang, X. Lu, D. Niyato, P. Wang, and D. I. Kim, "Ambient backscatter communications: A contemporary survey," *IEEE Commun. Surveys Tuts.*, vol. 20, no. 4, pp. 2889–2922, Apr. 2018.
[13] D. Darsena, G. Gelli, and F. Verde, "Modeling and performance analysis of wireless networks with ambient backscatter devices," *IEEE Trans. Commun.*, vol. 65, no. 4, pp. 1797–1814, Jan. 2017.
[14] V. Liu, A. Parks, V. Talla, S. Gollakota, D. Wetherall, and J. R. Smith, "Ambient backscatter: wireless communication out of thin air," in *Proc. ACM SIGCOMM*, Aug. 2013, pp. 39–50.
[15] G. Wang, F. Gao, R. Fan, and C. Tellambura, "Ambient backscatter communication systems: Detection and performance analysis," *IEEE Trans. Commun.*, vol. 64, no. 11, pp. 4836–4846, Nov. 2016.
[16] J. Qian, F. Gao, G. Wang, S. Jin, and H. Zhu, "Noncoherent detections for ambient backscatter system," *IEEE Trans. Wireless Commun.*, vol. 16, no. 3, pp. 1412–1422, Mar. 2017.
[17] H. Guo, Q. Zhang, S. Xiao, and Y. C. Liang, "Exploiting multiple antennas for cognitive ambient backscatter communication," *IEEE Internet Things J.*, vol. 6, no. 1, pp. 765–775, Feb. 2019.
[18] D. T. Hoang, D. Niyato, P. Wang, D. I. Kim, and Z. Han, "Ambient backscatter: A new approach to improve network performance for RF-powered cognitive radio networks," *IEEE Trans. Commun.*, vol. 65, no. 9, pp. 3659–3674, Sep. 2017.
[19] D. Li, W. Peng, and Y.-C. Liang, "Hybrid ambient backscatter communication systems with harvest-then-transmit protocols," *IEEE Access*, vol. 6, pp. 45288–45298, 2018.
[20] B. Lyu, H. Guo, Z. Yang, and G. Gui, "Throughput maximization for hybrid backscatter assisted cognitive wireless powered radio networks," *IEEE Internet Things J.*, vol. 5, no. 3, pp. 2015–2024, Jun. 2018.
[21] B. Lyu, C. You, Z. Yang, and G. Gui, "The optimal control policy for RF-powered backscatter communication networks," *IEEE Trans. Veh. Technol.*, vol. 67, no. 3, pp. 2804–2808, Mar. 2018.
[22] X. Lu, H. Jiang, D. Niyato, D. I. Kim, and Z. Han, "Wireless-powered device-to-device communications with ambient backscattering: Performance modeling and analysis," *IEEE Trans. Wireless Commun.*, vol. 17, no. 3, pp. 1528–1544, Mar. 2018.
[23] G. Yang, Y.-C. Liang, R. Zhang, and Y. Pei, "Modulation in the air: Backscatter communication over ambient OFDM carrier," *IEEE Trans. Commun.*, vol. 66, no. 3, pp. 1219–1233, Mar. 2018.

[24] G. Yang, Q. Zhang, and Y. C. Liang, "Cooperative ambient backscatter communications for green Internet-of-Things," *IEEE Internet Things J.*, vol. 5, no. 2, pp. 1116–1130, Apr. 2018.
[25] R. Correia, D. Belo, F. Pereira, M. Jordão, and N. B. Carvalho, "Backscatter modulation for wearable devices: A backscatter modulator, consisting of an antenna and a 1-MHz binary backscatter modulator operating at a carrier frequency of 915 MHz," *IEEE Microw. Mag.*, vol. 20, no. 1, pp. 78–84, Jan. 2019.
[26] Q. Zhang, H. Guo, Y. C. Liang, and X. Yuan, "Constellation learning-based signal detection for ambient backscatter communication systems," *IEEE J. Sel. Areas Commun.*, vol. 37, no. 2, pp. 452–463, Feb. 2019.
[27] W. Liu, Y. C. Liang, Y. Li, and B. Vucetic, "Backscatter multiplicative multiple-access systems: Fundamental limits and practical design," *IEEE Trans. Wireless Commun.*, vol. 17, no. 9, pp. 5713–5728, Sep. 2018.
[28] S. N. Daskalakis, R. Correia, G. Goussetis, M. M. Tentzeris, N. B. Carvalho, and A. Georgiadis, "Four-PAM modulation of ambient FM backscattering for spectrally efficient low-power applications," *IEEE Trans. Microw. Theory Techn.*, vol. 66, no. 12, pp. 5909–5921, Dec. 2018.
[29] J. Qian, A. N. Parks, J. R. Smith, F. Gao, and S. Jin, "IoT communications with M–PSK modulated ambient backscatter: Algorithm, analysis, and implementation," *IEEE Internet Things J.*, vol. 6 no. 1, pp. 844–855, Feb. 2018.
[30] R. Correia, A. Boaventura, and N. B. Carvalho, "Quadrature amplitude backscatter modulator for passive wireless sensors in IoT applications," *IEEE Trans. Microw. Theory Techn.*, vol. 65, no. 4, pp. 1103–1110, Apr. 2017.
[31] G. D. Forney, Jr., and G. Ungerboeck, "Modulation and coding for linear Gaussian channels," *IEEE Trans. Inf. Theory*, vol. 44, no. 6, pp. 2384–2415, Oct. 1998.
[32] S. Boyd and L. Vandenberghe, *Convex Optimzation*. Cambridge, U.K.: Cambridge Univ. Press, 2004.
[33] R. E. Blahut, *Principles and Practice of Information Theory*. Boston, MA, USA: Addison-Wesley, 1987.
[34] A. L. Yuille and A. Rangarajan, "The concave-convex procedure," *Neural Comput.*, vol. 15, no. 4, pp. 915–936, 2003.
[35] R. G. Bland, D. Goldfarb, and M. J. Todd, "The ellipsoid method: A survey," *Operations Res.*, vol. 29, no. 6, pp. 1039–1091, 1981.
[36] A. J. Goldsmith and P. P. Varaiya, "Capacity of fading channels with channel side information," *IEEE Trans. Inf. Theory*, vol. 43, no. 6, pp. 1986–1992, Nov. 1997.
[37] S. M. Moser, "Some expectations of a non-central chi-square distribution with an even number of degrees of freedom," in *Proc. IEEE TENCON*, Nov. 2007, pp. 1–6.
[38] I. S. Gradshteyn and I. M. Ryzhik, *Table of Integrals, Series, and Products*. New York, NY, USA: Academic, 2014.

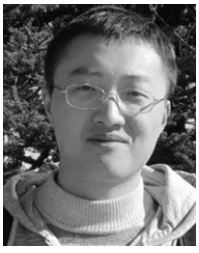

HUAYAN GUO (M'18) received the B.S. degree in electronic information science and technology from the Beijing University of Posts and Telecommunications, Beijing, China, in 2012, and the Ph.D. degree from Peking University, Beijing, in 2017. He is currently a Postdoctoral Researcher with the Center for Intelligent Communications and Networking (CINC), University of Electronic Science and Technology of China. His research interests include cognitive radio and the Internet-of-Things communications.

YING-CHANG LIANG (F'11) was a Professor with The University of Sydney, Australia, a Principal Scientist and a Technical Advisor with the Institute for Infocomm Research, Singapore, and a Visiting Scholar with Stanford University, USA. He is currently a Professor with the University of Electronic Science and Technology of China, China, where he leads the Center for Intelligent Networking and Communications and is the Deputy Director of the Artificial Intelligence Research Institute. His research interests include wireless networking and communications, cognitive radio, dynamic spectrum access, the Internet of Things, artificial intelligence, and machine-learning techniques.

Dr. Liang has been recognized by Thomson Reuters (currently Clarivate Analytics) as a Highly Cited Researcher, since 2014. He was a recipient of numerous paper awards, including the IEEE Jack Neubauer Memorial Award, in 2014, and the IEEE Communications Society APB Outstanding Paper Award, in 2012. He received the Prestigious Engineering Achievement Award from The Institution of Engineers, Singapore, in 2007, the Outstanding Contribution Appreciation Award from the IEEE Standards Association, in 2011, and the Recognition Award from the IEEE Communications Society Technical Committee on Cognitive Networks, in 2018. He is the Founding Editor-in-Chief of the IEEE JOURNAL ON SELECTED AREAS IN COMMUNICATIONS: COGNITIVE RADIO SERIES, and the Key Founder and the Editor-in-Chief of the IEEE TRANSACTIONS ON COGNITIVE COMMUNICATIONS AND NETWORKING. He is also serving as an Associate Editor-in-Chief for *China Communications*. He served as a Guest/Associate Editor for the IEEE TRANSACTIONS ON WIRELESS COMMUNICATIONS, the IEEE JOURNAL OF SELECTED AREAS IN COMMUNICATIONS, *IEEE Signal Processing Magazine*, the IEEE TRANSACTIONS ON VEHICULAR TECHNOLOGY, and the IEEE TRANSACTIONS ON SIGNAL AND INFORMATION PROCESSING OVER NETWORKS. He was also an Associate Editor-in-Chief of the *World Scientific Journal on Random Matrices: Theory and Applications*. He was a Distinguished Lecturer of the IEEE Communications Society and the IEEE Vehicular Technology Society. He was the Chair of the IEEE Communications Society Technical Committee on Cognitive Networks. He served as the TPC Chair and as the Executive Co-Chair for the IEEE GLOBECOM 2017.

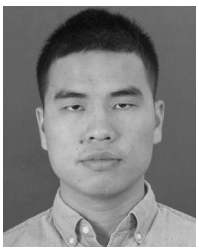

RUIZHE LONG (S'17) received the B.S. degree in communication engineering from the University of Electronic Science and Technology of China (UESTC), China, in 2017, where he is currently pursuing the Ph.D. degree. His research interests include backscatter communication and the Internet of Things. He was a recipient of the IEEE GLOBECOM 2017 Student Travel Grant Award.

SA XIAO (M'18) received the B.S.E., M.S.E., and Ph.D. degrees from the University of Electronic Science and Technology of China, Chengdu, China, in 2009, 2012, and 2017, respectively. In 2015, he was a Visiting Student with the Department of Electrical and Computer Engineering, Southern Illinois University, Carbondale, IL, USA. He was also a Visiting Student with the Division of Electrical and Computer Engineering, Louisiana State University, Baton Rouge, LA, USA, from 2015 to 2017. He is currently a Postdoctoral Researcher with the Center for Intelligent Communications and Networking (CINC), University of Electronic Science and Technology of China. His research interests include device-to-device communications, full-duplex communications, heterogeneous networks, and the Internet-of-Things communications.

QIANQIAN ZHANG (S'17) received the B.S. degree in communication engineering from Jilin University, in 2016. She is currently pursuing the Ph.D. degree with the University of Electronic Science and Technology of China (UESTC), China. Her research interests include transceiver design for the Internet of Things, and machine learning for wireless communications.